Study on the role of the reaction time in the upcycling of HDPE by co-hydrocracking it with VGO

Francisco J. Vela [a], Roberto Palos [a,b], Suní Rodríguez [a], M. Josune Azkoiti [b], Javier Bilbao [a], Alazne Gutiérrez [a,*]

[a] *Department of Chemical Engineering, University of the Basque Country UPV/EHU, PO Box 644, 48080 Bilbao, Spain*
[b] *Department of Chemical and Environmental Engineering, University of the Basque Country UPV/EHU, Plaza Ingeniero Torres Quevedo 1, 48013 Bilbao, Spain*

ABSTRACT

Pursuing the aim of improving the current waste plastics management strategy, we have investigated the co-hydrocracking of high-density polyethylene (HDPE) with vacuum gasoil (VGO) over a PtPd/HY catalyst for converting this blend into high-quality fuels. In particular, the work was focused on assessing the effects of the reaction time on the product yields and on the composition of the gas, naphtha and light cycle oil (LCO) fractions, which was determined by chromatographic means. The experimental runs were carried out in a 100 mL semi continuous stirred tank reactor varying the reaction time between 15 and 120 min and maintaining constant the rest of the variables at 420 °C (temperature reached using an electrical heating jacket and following a 5 °C min^{-1} heating ramp), 80 bar and a catalyst to oil mass ratio of 0.075 $g_{cat}\, g_{oil}^{-1}$. The results shown that at 120 min a naphtha fraction rich in 1-ring aromatics and with a RON value of 92.5 was obtained, while the LCO fraction was mainly iso-paraffinic with a cetane index of 43.8. Hence, these fractions could be used in the corresponding blending stages of commercial gasoline and diesel. Furthermore, the coke deposited on the catalyst was analyzed by means of TPO, obtaining that it was mainly formed at short contact times (< 15 min) and that its nature evolved with contact time being less condensed at long contact times.

1. Introduction

Global plastic generation has increased restlessly in the last decades, reaching a value of 353 Mtons in 2020 [1]. However, the waste management and recycling strategies continue to fall short. Indeed, the poor development of the recycling industries has caused that more than 90% of the waste plastics ever generated have ended landfilled, incinerated or dispersed in a natural environment once their life cycle has reached its end [2]. As a consequence of this mismanagement, the massive accumulation of plastic debris in terrestrial and aquatic environments has occurred, leading to its degradation and fragmentation into microplastics. In this way, the pollution caused by microplastics is of particular concern given the long-lasting nature and the widespread presence of these particles [3]. Furthermore, the emergence of COVID-19 disease has brought a huge consumption of single-use plastic-made healthcare and personal protection equipment, the valorization of which requires the establishment of appropriate strategies [4]. The pandemic has also delayed the politics of the developed countries directed to cap global

plastic production [5] and to replace the conventional plastic made from fossil fuels (99% of the current production) with other biodegradable materials [6]. Hence, the recycling of waste plastics is a huge challenge for modern humankind considering the severe environmental and health issues derived from their mismanagement.

It should be highlighted that the plastic recycling technologies, in particular thermochemical processes (pyrolysis, gasification, catalytic cracking and hydrocracking), have acquired an important maturity level given their versatility and scaling-up capacity [7–9]. The aim has been mainly focused on the production of fuels or raw chemicals by means of selective processes that require the use of catalysts [10]. Palos et al. [11] analyzed the difficulties for the installation of new industries for the production of high-quality fuels (gasoline and diesel) and their subsequent commercialization. Consequently, they proposed that the best strategy for solving in the short-term the severe problem of waste plastic stock is involving oil-refineries in the plastics recycling chain (Waste Refinery) within the Circular Economy framework. The alternative strategies that a Waste Refinery can offer are: (i) the direct co-feeding of

the waste plastics to already existing units; (ii) the co-feeding of plastic pyrolysis oil (PPO) with benchmark feedstock; and (iii) the installation of new *ad hoc* designed valorization units. Moreover, the fuels and secondary products obtained in a Waste Refinery could be entirely valorized and their composition would be adapted using the separation and reforming units available in refineries (usually already depreciated units), easing their subsequent commercialization. Among the units available in refineries for valorizing waste plastics, the most attractive ones for the co-feeding are the fluid catalytic cracking (FCC) [12,13] and the hydrocracking units [14].

Hydrocracking is a key process so that oil refineries can cover the increasing demand for fuels and petrochemicals from ever more heavy crude, with a large number of contaminants (S, N, metals, asphaltenes) and producing a higher yield of distillation residue [15]. Based on their high versatility, hydrocracking units are considered appropriate for the production of fuels from alternative feeds, such as bio-oil (liquid product obtained in the fast pyrolysis of biomass) and residua from the consumers society [16]. The valorization of waste plastics would allow to intensify the valorization of oil, taking into account that currently more than 9 wt% of oil is used in the production of plastics [17]. In addition to the environmental advantages of recycling waste plastics, with the use of hydrocracking units, the fuels produced would comply with the legal requirements for a limited environmental impact in their combustion. In this sense, the recovery in a refinery, which already has the appropriate and depreciated equipment, also facilitates the minimization of greenhouse gas emissions generated in the production of fuels.

Munir et al. [18] reviewed the recent advances in the study of hydrocracking catalysts, focusing on the effects of the operating conditions (temperature, hydrogen pressure, reaction time) on the conversion, yield and composition of the fuels obtained in the hydrocracking of different plastics. The experimentation has been commonly performed in stirred batch reactors, with values of temperature and hydrogen pressure within the ranges of 300–450 °C and 2–15 MPa, respectively. Furthermore, hydrocracking shows important advantages for the production of fuels with respect to other polyolefins valorization alternatives. Among them, it should be highlighted that: (i) the overcracking, which is a usual phenomenon in riser FCC units, is inhibited. In this way, an excessive production of C_1-C_4 gaseous products is restricted [19]; and (ii) the bifunctional catalysts used in hydrocracking boost both the cracking and the isomerization reactions, producing high yields of iso-paraffinic gasoline [20,21]. The mechanism occurs through carbenium ions for highly acidic catalysts, but for weak acid sites, the free radical mechanism is the most predominant one. Vance et al. [22] explained the formation of iso-paraffins in the hydrocracking of LDPE over a Pt-WZr catalyst by the preferential adsorption of polymer chains and their partial isomerization prior to cracking. In this mechanism, the metal-to-acid site molar ratio of the catalyst has a relevant role in the distribution and isomerization degree of the products. Kots et al. [23] compared the conditions and selectivity of the products obtained in the hydrocracking and in the hydrolysis of polyolefins, highlighting the lower energy demand of the hydrocracking process.

In this work, the hydrocracking of a blend of high density polyethylene (HDPE) and vacuum gas oil (VGO) over a PtPd/HY catalyst has been investigated. Paying special attention to the effects of the reaction time on the conversion of both feeds and on the distribution and composition of the products. The aim of the work is to progress towards the knowledge of the ideal operating conditions for the co-feeding of waste plastics with a refinery stream, which is a reference feedstock for hydrocracking units due to its high aromaticity. The hydrocracking of VGO has been extensively studied in the literature, using different bifunctional catalysts [24], but not the joint hydrocracking of polyolefins and VGO. In a previous work [25] we assessed the effects of co-feeding HDPE (20 wt%) with VGO obtaining that the co-feeding increased the conversion of VGO and boosted the formation of naphtha. Furthermore, it was established that 420 °C was the appropriate temperature for maximizing the HDPE conversion without

obtaining an excessive overcracking of the naphtha fraction. In a subsequent work [26], we determined the importance of H_2 pressure on the distribution and composition of the products. It was obtained that operating at 80 bar the composition of the fractions obtained was similar to that of refinery gasoline and diesel. This work is a continuation of the previous ones. This time, the evolution of the distribution and composition of the products with the contact time of the catalyst has been established. In addition, the coke deposited on the catalyst has been studied, complementing the knowledge of this process and offering information of interest to develop a strategy for co-feeding waste plastics into refinery hydrocracking units.

2. Experimental

2.1. Materials

The vacuum gasoil (VGO) was provided by Petronor S.A. refinery (Muskiz, Spain). It consisted of a mixture of the heavy gasoils produced in the vacuum distillation, visbreaker and coker units available in the refinery. Besides, as the VGO is commonly used in the refinery as the benchmark feedstock of the fluid catalytic cracking (FCC) unit, it was hydrotreated within the refinery facilities to reduce its contents of sulfur and nitrogen. The main physicochemical properties of the VGO have been displayed in Table 1. An in-detail explanation of the techniques and procedures followed for its characterization can be found elsewhere [26]. In short, it was a heavy stream (boiling range of 314–519 °C) with low contents of heteroatoms (510 and 305 ppm of sulfur and nitrogen, respectively), which minimized the poisoning of the supported noble metals of the catalyst. Furthermore, it should be highlighted its high content of aromatic compounds (48.4 wt%), in which the contribution of poly-aromatics was quite remarkable (15.8 wt%).

The high-density polyethylene (HDPE) was purchased from Dow Chemical (Tarragona, Spain). Its main properties, which have been provided by the supplier, have been also related in Table 1. Before being used, the pellets of HDPE were grinded at cryogenic conditions to reduce their size (< 100 μm).

A PtPd/HY catalyst (particle size 125–350 μm) was used for the HDPE/VGO blend hydrocracking. The catalyst was synthesized in our facilities following the procedure shown in Fig. S1. In essence, the HY zeolite (CBV712, supplied by Zeolyst International) was calcined at

Table 1
Physical and chemical properties of the feeds.

	VGO	HDPE
Physical properties		
density at 25 °C (g mL^{-1})	0.8912	0.9403
viscosity at 37.8 °C (cSt)	34.2	–
average molecular weight (g mol^{-1})	377	46,200
higher heating value (MJ kg^{-1})	45	43
Simulated distillation (°C)		
IBP−FBP	314−519	–
T_{50} −T_{95}	415−491	–
Distillation fractions (wt%)		
naphtha (< 216 °C)	0.17	–
LCO (216–350 °C)	4.48	–
HCO (> 350 °C)	95.4	–
Elemental analysis (wt%)		
C	87.3	85.7
H	12.5	14.3
N	305[a]	–
O	–	–
S (ppm)	510[b]	–
Composition (wt%)		
paraffins	14.0	–
naphthenes	35.3	–
olefins	–	–
1−ring aromatics	20.3	–
2−ring aromatics	12.4	–
3$^+$−ring aromatics	15.8	–

550 °C (heating rate of 5 °C min^{-1}) to obtain its acidic form. Next, the HY zeolite was suspended in distilled water at 80 °C and pH = 7 to enhance the electrostatic attraction. Then, noble metals were incorporated from aqueous solutions of Pt(NH$_3$)$_4$(NO$_3$)$_2$ and Pd(NH$_3$)$_4$(NO$_3$)$_2$, both purchased from Sigma-Aldrich. Once adsorption equilibrium was reached (~24 h), the excess of water was removed in a rotary vacuum evaporator at 80 °C. After that, the catalyst was dried overnight at 110 °C and, finally, it was calcined at 450 °C for 2 h (heating rate of 5 °C min^{-1}). Subsequently, the catalyst was characterized through several techniques and obtained results were related in Table S1 in Supplementary Material. A description of the procedures was already provided [25]. Briefly, it has a metal content of 1.19 wt% of Pt and 0.53 wt% of Pd measured by ICP-AES. The TEM image (Fig. S2) shows that PtPd metallic sites are well dispersed on the surface of the HY zeolite. From the N$_2$ adsorption-desorption isotherms it was obtained that the specific surface of the catalyst is of 620 m^2 g^{-1}, with a remarkable contribution of the micropores (543 m^2 g^{-1}). Regarding its acidic properties, the total acidity and average strength of the catalyst (1.69 mmol g^{-1} and 135 kJ mol^{-1}, respectively) were obtained by means of a *tert*-butyl amine temperature programmed desorption, whereas the Brønsted to Lewis acidic sites ratio (1.53) was determined by pyridine FTIR analysis. The HY zeolite was chosen as the support because its good properties in terms of acidity and specific surface area ensure a good performance in the hydrocracking of the stream used in this work.

2.2. Experimental unit and product analysis

The blend used for the hydrocracking tests was composed of 20 wt% of HDPE and 80 wt% of VGO. The operation took place in a 100 mL stainless steel stirred tank semi-batch reactor system from PID Engineering & Tech. (schematic diagram available in Fig. S3). The reactor system was also equipped with other auxiliary items, such as two gas cylinders (N$_2$ and H$_2$) connected to a gas mass flow control system, a temperature controller that acted over an electrical heating jacket and a control pressure valve, among others [25]. The reactor vessel was loaded with both fresh catalyst (3 g) and feed (40 g of the HDPE/VGO blend) and, after performing a leak test to ensure that the reactor was airtight closed, it was heated up to 420 °C following a heating ramp of 5 °C min^{-1} and pressurized at 80 bar with pure H$_2$. The pressure was kept constant at 80 bar by establishing a continuous hydrogen flow (200 mL min^{-1}). The stirring was activated once the desired operating conditions were reached, establishing that very moment as zero time.

Since the aim of the work was to assess the effects of the reaction time, this parameter was varied within the range of 15–120 min, whereas the rest of the parameters were maintained constant at the following values: 420 °C (measured with a K type thermocouple), 80 bar (regulated with a PID controller), catalyst to oil mass ratio of 0.075 g$_{cat}$ g$_{oil}^{-1}$ and stirring rate of 1300 rpm. These values were established based on the results obtained in our previous works, since they ensured good yields of naphtha and LCO fractions with compositions similar to those of the industrial fractions [25–27].

Prior to the hydrocracking reactions, the PtPd/HY catalyst was reduced *ex-situ* in a fixed bed reactor at 400 °C for 4 h using a 80 mL min^{-1} stream of H$_2$ diluted in N$_2$ (0.375 vol ratio) to ensure the total activation of the metallic sites.

The gases leaving the reactor were cooled in a double pipe condenser and the lightest fraction (C$_1$-C$_4$) was collected in a gas sampling bag to be analyzed. The gas fraction was analyzed by chromatographic means in an Agilent 6890 GC equipped with an FID detector and a HP-PONA column (50 m × 0.2 mm × 0.5 μm).

The liquid products were separated from the unconverted HDPE (which has been denoted as wax from this point on) and the spent catalyst by following a two-stage solvent fractionation method [25]. The methodology has been summarized in Fig. S4. In short, the first stage was performed at room temperature and using tetrahydrofuran as extracting agent to remove the hydrocarbons from the products. While

in the second step, the wax was separated from the spent catalyst operating at 130 °C and using xylene as solvent. Finally, spent catalyst was dried in an oven at 150 °C for 24 h to ensure that xylene was totally removed. Afterwards, to fully characterize the composition of the liquid products, they were submitted to various analyses. Firstly, the boiling range distribution of the liquid products was analyzed following the procedure described in the ASTM D2887 Standard. It was used an Agilent 6890 GC chromatograph provided with an FID detector and a DB-2887 semi-capillary column (10 m × 0.53 mm × 3.00 μm). This analysis allowed to lump the liquid products in the following fractions: naphtha (C$_5$-C$_{12}$), light cycle oil (LCO, C$_{13}$-C$_{20}$) and heavy cycle oil (HCO, C$_{21+}$). Secondly, the PIONA composition of the naphtha and LCO fractions was obtained by comprehensive chromatography in combination with mass spectrometry (GC×GC/MS). The equipment and its configuration have been explained in previous works [14,25]. Thirdly, the research octane number (RON) of the naphtha fraction was calculated from gas chromatographic data as described by Anderson et al. [28]. Fourthly, the cetane index of the LCO fraction was computed according to the ASTM D4737 Standard.

The coke deposited on the catalyst was analyzed by means of temperature programmed oxidation (TPO) analysis in a TA Instruments TGA-Q 5000 thermobalance. The procedure followed for the analysis corresponds has been widely reported in the literature for characterizing the coke produced in the upgrading of hydrocarbon streams [29].

2.3. Reaction indices

For evaluating the extent of the hydrocracking reactions, different reaction indices were defined. Since the feed used was a blend of HDPE and VGO, a conversion index was defined for describing the conversion of each one. The conversion of VGO, was evaluated in terms of the disappearance of its heaviest fraction, the HCO fraction, which represents 95.4 wt% of its composition (Table 1):

$$\text{VGO conversion:} \quad X_{HCO} = \frac{(m_{HCO})_{initial} - (m_{HCO})_{final}}{(m_{HCO})_{initial}} \cdot 100 \tag{1}$$

where $(m_{HCO})_{initial}$ is the mass of HCO fed into the system and $(m_{HCO})_{final}$ is the mass of HCO obtained after the reaction time.

The plastic conversion was defined as follows:

$$\text{HDPE conversion:} \quad X_{HDPE} = \frac{(m_{HDPE})_{initial} - (m_{HDPE})_{final}}{(m_{HDPE})_{initial}} \cdot 100 \tag{2}$$

where $(m_{HDPE})_{initial}$ is the mass of HDPE fed into the system and $(m_{HDPE})_{final}$ is the mass of HDPE (wax) obtained after the reaction time.

In addition, the yield of each product fraction was defined as the mass of fraction i formed to the total amount of feed:

$$Y_i = \frac{m_i}{(m_{VGO} + m_{HDPE})_{initial}} \cdot 100 \tag{3}$$

3. Results and discussion

3.1. Hydrocracking yield and conversion

Fig. 1 depicts the evolution with the reaction time of the distribution of product yields, together with the HCO and HDPE conversions (X_{HCO} and X_{HDPE}, respectively). Attending to the evolution of both types of conversion, it can be seen how different the reaction rates of the HCO and the HDPE were. In this way, the HDPE reacted very slowly, while the hydrocracking rate of the VGO was very fast. Focusing on the latter, within 15 min of reaction the yield of the HCO fraction decreased from 76.2 to 33.6 wt% (X_{HCO} = 55.9%) and continued decreasing gradually for 90 min (20.4 wt%). From this point on, a pseudo-stable state was reached and the same HCO conversion value was obtained at 90 and 120 min (73.2%) value. It has to be mentioned that the cracking of the
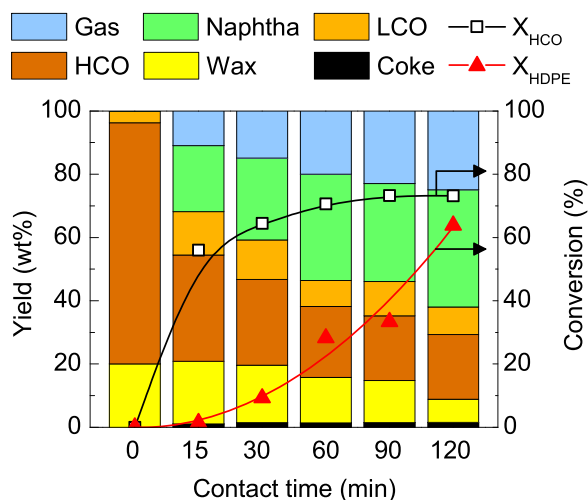
Fig. 1. Evolution with the reaction time of the product yields and conversions.

HDPE chains produced C_{13+} molecules that were quantified within the LCO and HCO fractions, contributing to the global result of an almost constant HCO conversion above 90 min [30]. In contrast, the yield of naphtha increased continuously, going from 20.9 wt% at 15 min to 36.9 wt% at 120 min. Similarly, the production of gases increased with the reaction time, reaching a final yield of 25 wt% at 120 min. The yield of coke also increased from 1.1 to 1.6 wt% at 15 and 120 min, respectively, which exposed that the deposition of coke was such a fast phenomenon.

As aforementioned, the initial hydrocracking rate of the HDPE was negligible compared to that of the VGO. In this way, the HDPE conversion was almost null at 15 min and it remained in moderate values (9.2%) at 30 min. From this point on, X_{HDPE} increased up to 28.2 % at 60 min and reached a final value of 63.9% at 120 min. This evolution of the HDPE conversion with reaction time was in concordance with that previously obtained by Pan et al. [30] in the hydrocracking of HDPE at 400 °C, 1 MPa of H_2 and using a NiMo/Al_2O_3 catalyst. Equally, Ali et al. [31] reported an increase in the conversion from 30.6 % to 86.9% in the 30–60 min range in the hydrocracking of a blend composed of LDPE and petroleum resid operating at 430 °C, 1220 psig of H_2 and using a NiMo/γ-Al_2O_3 catalyst. Previously, Joo et al. [32] also obtained a qualitatively similar evolution for the plastic conversion in the hydrocracking of a ternary blend composed of LDPE, coal and petroleum resid working at 430 °C, 8.3 MPa of H_2 and using a NiMo/Al_2O_3 catalyst.

The different hydrocracking rate of the HDPE and the VGO can be mainly attributed to the limitations that the HDPE molecules faced in the catalytic cracking, since they must undergo through thermal cracking to reduce the HDPE chains to smaller compounds capable of diffusing to the inner porous structure of the catalyst. To evaluate the role of the catalyst, Fig. S5 compares, under the same operating conditions, the results of hydrocracking VGO and HDPE/VGO blend without catalyst with those obtained in the hydrocracking of HDPE/VGO blend with catalyst. As it can be seen, the use of the catalyst is required to promote the conversion of HDPE and VGO into liquid fuels (naphtha and LCO) and gases.

3.2. Gas products

The evolution with the reaction time of the composition of the gas products obtained in the hydrocracking of the HDPE/VGO blend has been displayed in Fig. 2. A clear predominance of the C_3 and the C_4 compounds was obtained for all the reaction times, which exposed that the predominant hydrocracking mechanism is that of carbenium ion reaction [33]. Note that light olefins were not detected at any reaction time given the high hydrogenation activity of the metals in the catalyst.
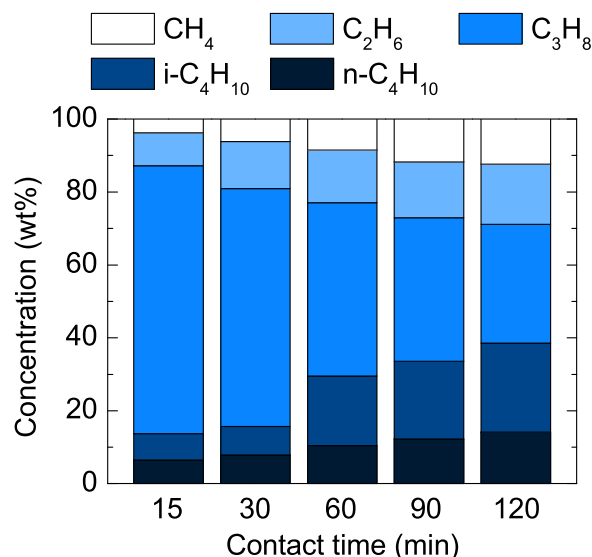

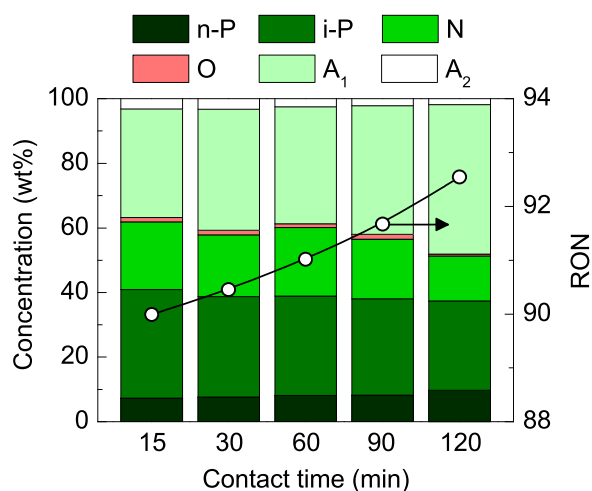**Fig. 2.** Evolution with the reaction time of the gas composition.

Indeed, pressures above 20 bar are enough to completely hydrogenate the light olefins [26]. At 15 min, gases were mainly formed by propane (73.6 wt%), small amounts of C_4 paraffins (13.7 wt%) and ethane (9 wt %) and methane in such a low concentration (3.7 wt%). Attending to the trend followed by the different compounds, it can be seen that methane, ethane and iso-butane followed remarkably increasing trends, while propane decreased with reaction time. Therefore, at 120 min the concentration of methane and ethane in the gases increased up to 12.4 and 16.5 wt%, respectively. Both the concentration of n- and iso-butane also increased (14.2 and 24.4 wt%, respectively), being the growth of the latter by far more remarkable. However, propane remained as the most abundant compound (32.6 wt%), in spite of the increasing trends of the rest of compounds.

It should be remarked that for 60 min onwards the concentration of the iso-butane underwent a notably increase, which coincided with the boosting experienced by the HDPE conversion (Fig. 1). Thus, it can be concluded that the dissolved HDPE macromolecules have suffered not only β–scission reactions, but also isomerization reactions in the acidic sites of the catalyst. In addition, catalyst deactivation will have a marked impact on these results, since the loss of activity will promote the formation of gas products by means of thermal cracking.

3.3. Naphtha fraction

The naphtha fraction obtained at each reaction time was characterized according to PIONA (paraffins, iso-paraffins, olefins, naphthenes and aromatics) analysis (Fig. 3). Note that olefinic compounds were detected in the naphtha fraction, since they were primary products obtained in the cracking of the HDPE chains, the hydrogenation of which is harder than that of C_2-C_4 olefins. Nonetheless, the concentration of olefins detected was below 1.5 wt% for all the reaction times, exposing once again the high hydrogenation activity of the catalyst.

For a reaction time of 15 min, an aliphatic naphtha fraction was obtained, in which the concentration of n-paraffins, iso-paraffins and naphthenes accounted for 7.2, 33.9 and 20.9 wt%, respectively. Thus, the concentration of aromatics was of 36.7 wt%, being the mono-aromatics the predominant ones (33.6 wt%). At longer reaction times, it can be seen that the concentration of aliphatics was reduced, whereas that of total aromatics increased (note that the reduction of the concentration of A_2 aromatics has been absorbed by the increase in the A_1 aromatics). In this way, for a reaction time of 120 min the naphtha fraction was mainly aromatic (48.1 wt%), being clearly dominated by mono-aromatics (46.3 wt%) and with a small concentration of di-

Fig. 3. Evolution with the reaction time of the naphtha composition and of the RON index. Key: n-P, n-paraffins; i-P, iso-paraffins; N, naphthenes; O, olefins; A$_1$, 1-ring aromatics; A$_2$, 2-ring aromatics.

aromatics (1.8 wt%). Furthermore, the concentration of paraffins (n- and iso-paraffins), naphthenes and olefins at 120 min was of 37.3, 13.9 and 0.6 wt%, respectively. Nonetheless, in spite of the decreasing trend followed by the concentration of total paraffins, the concentration of linear paraffins increased from 7.2 to 9.7 wt% when increasing the reaction time from 15–120 min. Consequently, the concentration of ramified paraffins was reduced from 33.7 to 27.6 wt%, respectively. Similar trends were previously observed by Pan et al. [30] in the composition of the liquid product obtained in the hydrocracking of neat HDPE at 400 °C, 1 MPa and using a Ni/Al$_2$O$_3$ catalyst.

The aforementioned increase of the concentration of A$_1$ aromatics can be attributed to the hydrodearomatization (HDA) activity of the catalyst. In this way, the 2-ring aromatics within the naphtha fraction were partially hydrogenated, leading to the formation of 1-ring aromatics. Likewise, the polyaromatic compounds within the LCO fraction were also converted into A$_1$ compounds through HDA reactions, since benzene, toluene and xylenes are the main products obtained in HDA reactions [34]. Furthermore, the Brønsted acid sites of the catalyst (Table S1) played a key role in the mechanism of the HDA reactions, since the polarity of these acid-type sites promoted the adsorption of highly polar A$_2$ and A$_{3+}$ compounds [35].

The evolution with the reaction time followed by the RON has been also displayed in Fig. 3. The results show that quite high RON values were obtained for the whole range of reaction time studied. In this way, at 15 min the RON was of 89.9 and it increased up to 92.5 after 120 min. The increasing trend followed by the RON layed on the increasing concentration of aromatics and of iso-paraffins, since these types of compounds have a positive impact over RON. Moreover, as reaction time went by, the length of the HDPE chains decreased at the same time that the branching number increased, boosting both high RON values [36]. Vasile et al. [37] investigated the hydrocracking of the oil obtained in the pyrolysis of electric appliances obtaining a RON of 90.9 operating at 350 °C, 6.5 MPa and using a DHC-8 commercial catalyst. The lower RON values obtained by them can be attributed to the low concentration of iso-paraffins they had in their naphtha fraction, which undoubtedly played to the detriment of the RON.

To sum up, regarding the composition and the RON values of the naphtha fraction obtained, it can be concluded that this fraction is appropriate for being used in the blending of commercial gasoline in refineries. Thus, by properly blending this naphtha with other naphthas produced in conventional refinery units, a commercial gasoline that will comply with the European environmental policies can be produced.

3.4. LCO composition and cetane index

The evolution with reaction time of the PIONA composition of the LCO faction has been collected in Fig. 4. Note that: (i) the concentration of naphthenes was below 0.1 wt% in all the cases; and (ii) no olefins were detected, so these families of compounds were not included in this figure. It should be highlighted that the evolution with the reaction time followed by the concentration of the families of compounds within the LCO fraction followed opposite trends to those within the naphtha fraction (Fig. 3). At short reaction times (15 and 30 min) the composition obtained was quite similar, being the aromatic compounds the predominant ones. The average concentration of 1-, 2- and 3$^+$-ring aromatics was of 8.0, 43.2 and 7.1 wt%, respectively. Within the aliphatic compounds, iso-paraffins predominated over n-paraffins (33.8 vs. 7.9 wt %, respectively).

According to the aforementioned effect of reaction time on product yields (Fig. 1), the HDPE conversion was significantly boosted at 60 min. Thus, this boost in the conversion of the HDPE chains was reflected in the composition of the LCO fraction (Fig. 4). In this way, at 60 min the LCO fraction became more paraffinic (46.7 wt%) and less aromatic (53.3 wt%) than before, even though its nature was still aromatic. This change in the composition was by far more evident at 120 min, where the paraffins accounted for 56.6 wt% and the aromatics for 43.4 wt%. Two main factors contributed to obtain these results. Firstly, the conversion of the HDPE chains to lighter compounds, which were mostly long linear paraffins within the boiling range of the LCO fraction [38]. Indeed, it occurs in two consecutive steps as described by Pan et al. [39]. Initially, the polyethylene chains are depolymerized by random scissions, producing long alkenes as products. These shorter chains can diffuse into the micropores of the zeolite and access the acid and metallic active sites available on its surface. Afterward, these alkenes are converted to paraffins through a carbocationic mechanism given the high H$_2$ pressure available in the system [16]. In addition, the long and linear paraffinic chains produced in the hydrocracking of the HDPE were then isomerized through skeletal rearrangement and subsequently hydrocracked in the Brønsted acid sites of the catalyst [33].

Secondly, the HDA activity of the catalyst saturated the aromatics within the LCO fraction and promoted their subsequent cracking and ring opening to lighter molecules within the naphtha fraction [40]. The HDA mechanism implied a complex reaction system that depends on the properties of the catalyst, composition of the reaction medium, and reaction conditions. Karakhanov et al. [34] simplified the mechanism into the following reactions: (i) hydrogenation reactions (reversible), also
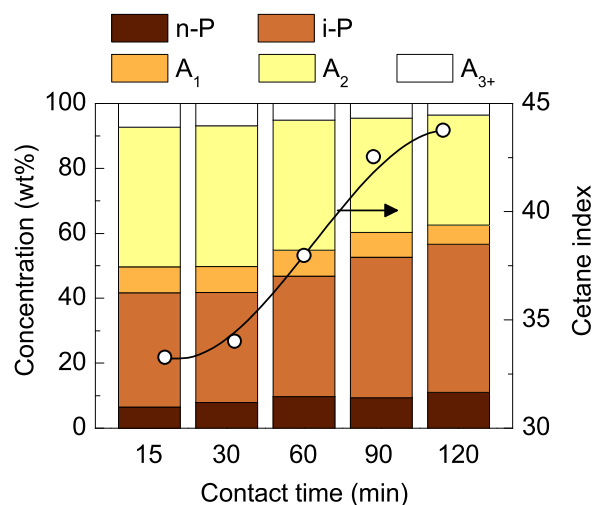
Fig. 4. Evolution with the reaction time of the LCO composition and of the cetane index. Key: n-P, n-paraffins; i-P, iso-paraffins; A$_1$, 1-ring aromatics; A$_2$, 2-ring aromatics; A$_{3+}$, 3$^+$-ring aromatics.

called saturation reactions; (ii) isomerization reactions (reversible), also called skeletal rearrangements; (iii) hydrocracking reactions, which are the C–C bond break reactions for the formation of new C–H bonds (ring opening reactions of the naphthenic rings are also considered); and (iv) dealkylation reactions, which are the C–C bond break reactions between benzene rings and substituent alkyl chains that result in the removal of the alkyl substituents. Thus, the aromatics within the LCO fraction, such as methylnaphthalene, acenaphthylene and pyrenes, were first converted into simpler aromatics by partially saturating them. It should be considered that some of the aromatics obtained as product in this first step of the HDA mechanism could be small enough to be part of the naphtha fraction. Then, these aromatics can undergo either isomerization, hydrocracking or dealkylation reactions, producing simple aliphatic compounds (especially paraffins and naphthenes) [41]. Furthermore, the monoaromatics and non-aromatic compounds can also interact with polyaromatics to produce well-structured coke [42].

Therefore, attending to the HDA mechanism of the VGO and considering that the HDPE chains went into depolymerization and hydrogenation reactions, long reaction times will promote the production of paraffinic LCO fractions. In addition, when the extent of HDPE hydrocracking in the HDPE/VGO blend progressed, the incidence in the product distribution was more important due to the competition of the alkenes coming from the HDPE against the VGO components to be adsorbed in the active sites of the catalyst.

The evolution of the cetane index of the LCO fraction with the reaction time has been also collected in Fig. 4. The cetane index is related to the composition of the LCO fraction sot that it is favored by the content of paraffins and inversely proportional to aromatics concentration [43]. By increasing reaction time, two simultaneous effects that tend to produce paraffinic compounds were promoted. On one hand, the HDA of the VGO compounds and, on the other hand, the depolymerization and cracking of the HDPE molecules. Thus, the cetane index showed a clear increasing trend that goes from 33.3 to 43.8 when increasing the reaction time from 15 m to 120 min. Moreover, at 60 min the cetane index increased abruptly (38.0) as a consequence of the aforementioned remarkable increase of the HDPE conversion (Fig. 1). The cetane index obtained was notably higher than that reported by Dagonikou et al. [44] in the hydrocracking of LCO, since they achieved a value of 32.0 operating at 380 °C, 1200 psig of H_2 and using a NiMo/-γ-Al_2O_3 catalyst.

According to the current European legislation (EN 590 Standard), commercial diesel must have a minimum cetane index of 46.0, which is a value slightly higher than those obtained for reaction times of 90 and 120 min (42.5 and 43.8, respectively). Therefore, the LCO fraction obtained in the hydrocracking of the HDPE/VGO blend cannot be directly used for feeding internal combustion engines, but it can be used in the blending stage of the commercial diesel pool in refineries.

Apart from the yield and composition of the naphtha and LCO fractions, the amount of the gas fraction formed at each reaction time must be also considered. Indeed, it could be a critical parameter since the gas fraction is totally composed of paraffins that lack of commercial interest, as they cannot be used as raw materials in the manufacture of chemical and polymer products. Therefore, this fact must be taken into account when selecting the optimal weight hourly space velocity to operate in a continuous hydrocracking reactor, which will be set according to the commercial interest of every single oil refinery.

3.5. Coke deposition

Fig. 5 shows the TPO profiles of the catalysts used in the hydrocracking of the HDPE/VGO blend for reaction times of 15, 60 and 120 min. In view of their shape, the TPO profiles were deconvoluted into two Gaussian peaks, allowing us to distinguish two types of coke: coke type I and coke type II. The former burnt at low temperature (375–400 °C), whereas the latter required higher temperatures (440–475 °C). The relation of combustion temperature with coke
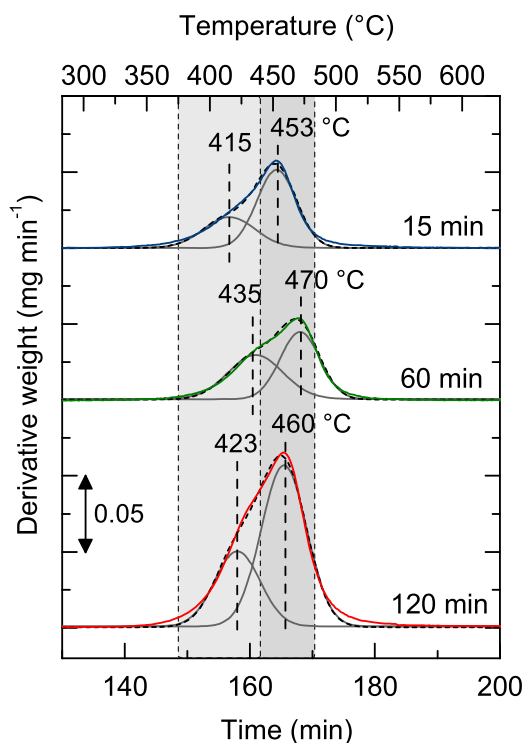

Fig. 5. TPO profiles of coke deposited in the catalyst for different reaction times.

location and nature was established according to previous works about the catalytic cracking of a blend of HDPE and VGO under FCC conditions [29], the hydrocracking of pyrenes on a NiW/Al catalyst [42] and the cracking of waste polyolefins [45].

The results obtained from the deconvolution of the TPO profiles have been summarized in Table 2, where the total content of coke, the maximum burning temperature (T_{Max}) and the content of each type of coke have been displayed. The evolution with reaction time of the total content of coke exposed that almost all the coke was formed in the first 30 min of reaction, since the growing rate of the coke for longer reaction times was by far smaller.

Analyzing the results obtained at 15 min (Fig. 5), coke type I had its maximum of combustion at 415 °C while coke type II at 453 °C. In addition, the area under the curve of coke type I was lower than that of coke type II, meaning that the content of the latter was higher (Table 2). Coke type I was presumably composed of depolymerized chains of HDPE (degraded macromolecules obtained in the initial cracking of the HDPE) and heavy molecules within the VGO that were retained on the surface of the catalyst. Considering that the conversion of HDPE into product fractions was negligible at 15 min (Fig. 1), it can be assumed that the contribution of long HDPE chains that cannot access the porous structure of the catalyst was quite relevant. However, it should be also taken into account that the metallic sites of the catalyst (PtPd) could catalyze the combustion of the coke and thus would contribute to lower the

Table 2
Deconvolution results of Gaussian peaks from the TPO profiles of the coke deposited in the used catalyst for different reaction times.

Reaction time (min)	15	60	120
Coke content (wt%)	14.9	18.8	21.2
Coke I			
$\quad T_{Max}$ (°C)	415	435	423
$\quad$ Content (wt%)	33.9	47.3	31.8
Coke II			
$\quad T_{Max}$ (°C)	453	470	460
$\quad$ Content (wt%)	66.1	52.7	68.2

combustion temperature [46]. The higher combustion temperature of coke type II was associated with the combustion of a coke with a lower H/C ratio and that was, presumably, placed inside of the porous structure of the catalyst [47]. In spite of being its combustion temperature higher than that of coke type I, it was indeed quite moderate ($T_{Max} < 480$ °C). This result exposed that, based on the classification established by Bauer and Karge [48], it was an amorphous and poorly structured coke. This fact can be attributed to the activity of the catalyst for the hydrocracking of the coke precursors that limited the condensation of these intermediate molecules and, especially, their development towards graphitic structures [49].

Comparing the results obtained at 60 min with those at 15 min, the TPO profiles were displaced towards higher temperatures (coke types I and II bunt at 435 and 470 °C, respectively). This result could be related to more condensed structures (lower H/C ratio) that were located more internally in the structure of the catalyst [50]. At this reaction time, coke type II continue to be the main one (52.7 wt% in Table 2). Furthermore, similarly to the coke formed at 15 min, the burning temperatures of the coke deposited at 60 min exposed that it was a low-developed coke [48].

At 120 min, the amount of coke deposited was bigger than that deposited in the previous reaction times. However, comparing the TPO profile with that obtained at 60 min, the maximum combustion temperatures were displaced to lower values for both types of coke (423 and 460 °C for coke types I and II, respectively). Thus, from 60 min onward, the coke did not continued condensing, but it was partially hydrogenated. This fact could be due to the hydrogen donor character of the HDPE molecules [51], which could contribute to reduce the aromaticity and to increase the H/C ratio of the coke. Furthermore, sharper profiles were obtained, which meant that the coke obtained at 120 min was less heterogeneous. Hence, it was a time long enough for the coke precursors and for the carbonaceous structures to evolve. In addition, the coke could be correlated with low-structured compounds based on the combustion temperatures of both types of coke [48].

To explain the commented effect of the reaction time on the content and characteristics of the coke, the change in the composition of the reaction medium must be also taken into account. According to the evolution with reaction time followed by the product yield and conversions (Fig. 1), the coke formed during the first 15 min of reaction would come from the hydrocracking of the VGO, since the HDPE conversion was very low ($X_{HDPE} < 2$ %). Besides, considering the aromatic nature of the VGO (Table 1) its hydrocracking would produce more developed structures [42], resulting in a displacement of its combustion temperature towards higher values at 60 min. For longer reaction times (120 min), the conversion of the HDPE was notably promoted and the composition of the coke will be modified and it will be burnt at lower temperatures (Table 2). This phenomenon lied in the modification of the composition of the reaction medium that would produce a coke fraction with a greater H/C ratio [49], also influenced by the hydrogen donor character of the degraded HDPE molecules [51]. Furthermore, for low values of HDPE conversion (reaction times below 60 min), the fraction of coke type I increased with reaction time, whereas that of coke type II decreased. Indeed, the amount of both types of coke were almost equal at 60 min (47.3 and 52.7 wt% for coke type I and type II, respectively). Nonetheless, extending the reaction time up to 120 min entailed an increase of the coke type II (up to 68.2 wt%), presumably because the alkenes formed in the decomposition of the HDPE were submitted to oligomerization and condensation reactions leading to the formation of polyaromatic structures. Those reactions were surely catalyzed by the acid sites of the zeolite and took place in parallel with the production of fuel-like molecules.

Furthermore, the stability of the catalyst was studied, using it in three successive reaction-regeneration cycles. The regeneration protocol consisted on two successive stages: i) sweeping with N_2 for 2 h at 400 °C; and, ii) coke combustion with air diluted in nitrogen for 19 h at 400 °C. The catalyst fully recovered its properties after regeneration and the results were reproduced in the successive reactions.

4. Conclusions

In the hydrocracking of the HDPE/VGO blend under the studied conditions (420 °C, 80 bar and using a PtPd/HY catalyst), the reactivity of the VGO and the HDPE is very different. Indeed, the reactivity of the HCO is quite fast since the very beginning, whereas that of the HDPE is not relevant until 60 min. Furthermore, the kinetics of both feeds is also different since the conversion of the VGO tends to a constant value (73.2 wt%) for times over 90 min, while that of HDPE increases exponentially with reaction time (65 wt% at 120 min). It should be highlighted the increase of the yield of naphtha with the reaction time (36.9 wt% at 120 min) but also an undesired increase of gas (25 wt%).

The effect of the reaction time over the composition of the gas, naphtha and LCO fractions is overall relevant. In the gas fraction, the concentration of propane decreases with reaction time and that of methane, ethane, n- and iso-butane increases. Furthermore, an increase in the reaction time promotes the formation of 1-ring aromatics in the naphtha fraction (46.3 wt% at 120 min), at the same time that the concentration of iso-paraffins and naphthenes decreases (13.9 and 27.6 wt%, respectively). Consequently, the RON value increases until reaching its maximum value of 92.5.

The LCO fraction is mainly composed of 2-ring aromatics and iso-paraffins, the concentration of which follows opposite trends. Thus, the concentration of the di-aromatics decreases with reaction time, but that of ramified paraffins increases, reaching final values of 43.4 and 33.8 wt%, respectively. As a consequence of the changes in composition, the cetane index increases, reaching its maximum value (43.7) at 120 min

The catalyst used shows an important content of coke (about 20 wt %), which is mainly deposited in the first 15 min of reaction. The TPO analysis exposes the existence of two fractions of coke (coke types I and II), which are deposited respectively on the external surface of the catalyst particles and inside of the micropores of the zeolite used as the support. Coke type I, which burns at a lower temperature, has been related to heavy components within the VGO and HDPE macromolecules retained in the catalyst. Coke type II is the main one and its content increases in parallel with the conversion of HDPE. This fact exposes the role of the hydrocarbons derived from the hydrocracking of HDPE in the formation of catalytic coke, which is catalyzed by the acid sites of the zeolite.

The results will serve to establish a solid basis to continue progressing to the co-feeding of waste plastics together with the benchmark feeds of the hydrocracking units. It will contribute to reach the goals of valorizing secondary refinery streams at the same time that the challenge of managing waste plastics rationally and at a large scale is solved.

CRediT authorship contribution statement

Francisco J. Vela: Investigation, Formal analysis, Writing – original draft. **Roberto Palos:** Formal analysis, Writing – original draft, Writing – review & editing, Visualization, Conceptualization. **Suní Rodríguez:** Investigation, Formal analysis. **M. Josune Azkoiti:** Methodology, Project administration, Visualization. **Javier Bilbao:** Writing – review & editing, Supervision, Project administration, Funding acquisition. **Alazne Gutiérrez:** Supervision, Methodology, Visualization, Conceptualization.

Declaration of Competing Interest

Data Availability

Data shown in the paper are property of the authors.

Acknowledgements

Appendix A. Supporting information

Supplementary data associated with this article can be found in the online version at doi:10.1016/j.jaap.2023.105928.

References

[1] OECD, Global Plastics Outlook, OECD, Paris, 2022, https://doi.org/10.1787/de747aef-en.

[2] I. Antonopoulos, G. Faraca, D. Tonini, Recycling of post-consumer plastic packaging waste in the EU: recovery rates, material flows, and barriers, Waste Manag. 126 (2021) 694–705, https://doi.org/10.1016/j.wasman.2021.04.002.

[3] K. Hu, Y. Yang, J. Zuo, W. Tian, Y. Wang, X. Duan, S. Wang, Emerging microplastics in the environment: properties, distributions, and impacts, Chemosphere 297 (2022), 134118, https://doi.org/10.1016/j.chemosphere.2022.134118.

[4] A.L. Patrício Silva, J.C. Prata, T.R. Walker, A.C. Duarte, W. Ouyang, D. Barceló, T. Rocha-Santos, Increased plastic pollution due to COVID-19 pandemic: challenges and recommendations, Chem. Eng. J. 405 (2021), 126683, https://doi.org/10.1016/j.cej.2020.126683.

[5] M. Bergmann, B.C. Almroth, S.M. Brander, T. Dey, D.S. Green, S. Gundogdu, A. Krieger, M. Wagner, T.R. Walker, A global plastic treaty must cap production, Science 376 (2022) (1979) 469–470, https://doi.org/10.1126/science.abq0082.

[6] V. Beghetto, R. Sole, C. Buranello, M. Al-Abkal, M. Facchin, Recent advancements in plastic packaging recycling: a mini-review, Materials 14 (2021) 4782, https://doi.org/10.3390/ma14174782.

[7] G. Lopez, M. Artetxe, M. Amutio, J. Alvarez, J. Bilbao, M. Olazar, Recent advances in the gasification of waste plastics. A critical overview, Renew. Sustain. Energy Rev. 82 (2018) 576–596, https://doi.org/10.1016/j.rser.2017.09.032.

[8] M. Solis, S. Silveira, Technologies for chemical recycling of household plastics – A technical review and TRL assessment, Waste Manag. 105 (2020) 128–138, https://doi.org/10.1016/j.wasman.2020.01.038.

[9] M.I. Jahirul, M.G. Rasul, D. Schaller, M.M.K. Khan, M.M. Hasan, M.A. Hazrat, Transport fuel from waste plastics pyrolysis – a review on technologies, challenges and opportunities, Energy Convers. Manag. 258 (2022), 115451, https://doi.org/10.1016/j.enconman.2022.115451.

[10] A. Eschenbacher, T. Myrstad, N. Bech, J.Ø. Duus, C. Li, P.A. Jensen, U. B. Henriksen, J. Ahrenfeldt, U.V. Mentzel, A.D. Jensen, Co-processing of wood and wheat straw derived pyrolysis oils with FCC feed—Product distribution and effect of deoxygenation, Fuel 260 (2020), 116312, https://doi.org/10.1016/j.fuel.2019.116312.

[11] R. Palos, A. Gutiérrez, F.J. Vela, M. Olazar, J.M. Arandes, J. Bilbao, Waste refinery: the valorization of waste plastics and end-of-life tires in refinery units. a review, Energy Fuels 35 (2021) 3529–3557, https://doi.org/10.1021/acs.energyfuels.0c03918.

[12] E. Rodríguez, A. Gutiérrez, R. Palos, F.J. Vela, M.J. Azkoiti, J.M. Arandes, J. Bilbao, Co-cracking of high-density polyethylene (HDPE) and vacuum gasoil (VGO) under refinery conditions, Chem. Eng. J. 382 (2020), 122602, https://doi.org/10.1016/j.cej.2019.122602.

[13] R. Palos, E. Rodríguez, A. Gutiérrez, J. Bilbao, J.M. Arandes, Cracking of plastic pyrolysis oil over FCC equilibrium catalysts to produce fuels: kinetic modeling, Fuel 316 (2022), 123341, https://doi.org/10.1016/j.fuel.2022.123341.

[14] D. Trueba, R. Palos, J. Bilbao, J.M. Arandes, A. Gutiérrez, Product composition and coke deposition in the hydrocracking of polystyrene blended with vacuum gasoil, Fuel Process. Technol. 224 (2021), 107010, https://doi.org/10.1016/j.fuproc.2021.107010.

[15] A. Marafi, H. Albazzaz, M.S. Rana, Hydroprocessing of heavy residual oil: opportunities and challenges, Catal. Today 329 (2019) 125–134, https://doi.org/10.1016/j.cattod.2018.10.067.

[16] J.W. Thybaut, G.B. Marin. Multiscale Aspects in Hydrocracking: From Reaction Mechanism Over Catalysts to Kinetics and Industrial Application, 1st ed., Elsevier Inc, 2016 https://doi.org/10.1016/bs.acat.2016.10.001.

[17] D. Whitehouse, Plastic recycling threatens oil demand growth, 2019.

[18] D. Munir, M.F. Irfan, M.R. Usman, Hydrocracking of virgin and waste plastics: a detailed review, Renew. Sustain. Energy Rev. 90 (2018) 490–515, https://doi.org/10.1016/j.rser.2018.03.034.

[19] F.J. Vela, R. Palos, D. Trueba, J. Bilbao, J.M. Arandes, A. Gutiérrez, Different approaches to convert waste polyolefins into automotive fuels via hydrocracking with a NiW/HY catalyst, Fuel Process. Technol. 220 (2021), 106891, https://doi.org/10.1016/j.fuproc.2021.106891.

[20] A. Bin Jumah, V. Anbumuthu, A.A. Tedstone, A.A. Garforth, Catalyzing the hydrocracking of low density polyethylene, Ind. Eng. Chem. Res 58 (2019) 20601–20609, https://doi.org/10.1021/acs.iecr.9b04263.

[21] A. bin Jumah, A.A. Tedstone, A.A. Garforth, Hydrocracking of virgin and post-consumer polymers, Microporous Mesoporous Mater. 315 (2021), 110912, https://doi.org/10.1016/j.micromeso.2021.110912.

[22] B.C. Vance, P.A. Kots, C. Wang, Z.R. Hinton, C.M. Quinn, T.H. Epps, L.T.J. Korley, D.G. Vlachos, Single pot catalyst strategy to branched products via adhesive isomerization and hydrocracking of polyethylene over platinum tungstated zirconia, Appl. Catal. B 299 (2021), 120483, https://doi.org/10.1016/j.apcatb.2021.120483.

[23] P.A. Kots, B.C. Vance, D.G. Vlachos, Polyolefin plastic waste hydroconversion to fuels, lubricants, and waxes: a comparative study, React. Chem. Eng. 7 (2022) 41–54, https://doi.org/10.1039/d1re00447f.

[24] B. Browning, P. Alvarez, T. Jansen, M. Lacroix, C. Geantet, M. Tayakout-Fayolle, A review of thermal cracking, hydrocracking, and slurry phase hydroconversion kinetic parameters in lumped models for upgrading heavy oils, Energy Fuels 35 (2021) 15360–15380, https://doi.org/10.1021/acs.energyfuels.1c02214.

[25] F.J. Vela, R. Palos, J. Bilbao, J.M. Arandes, A. Gutiérrez, Effect of co-feeding HDPE on the product distribution in the hydrocracking of VGO, Catal. Today 353 (2020) 197–203, https://doi.org/10.1016/j.cattod.2019.07.010.

[26] F.J. Vela, R. Palos, J. Bilbao, J.M. Arandes, A. Gutiérrez, Hydrogen pressure as a key parameter to control the quality of the naphtha produced in the hydrocracking of an HDPE/VGO blend, Catalysts 12 (2022) 543, https://doi.org/10.3390/catal12050543.

[27] F.J. Vela, R. Palos, D. Trueba, T. Cordero-Lanzac, J. Bilbao, J.M. Arandes, A. Gutiérrez, A six-lump kinetic model for HDPE/VGO blend hydrocracking, Fuel 333 (2023), 126211, https://doi.org/10.1016/j.fuel.2022.126211.

[28] P.C. Anderson, J.M. Sharkey, R.P. Walsh, Calculation of the research octane number of motor gasolines from gas chromatographic data and a new approach to motor gasoline quality control, J. Inst. Pet. 58 (1972) 83–94.

[29] E. Rodríguez, G. Elordi, J. Valecillos, S. Izaddoust, J. Bilbao, J.M. Arandes, P. Castaño, Coke deposition and product distribution in the co-cracking of waste polyolefin derived streams and vacuum gas oil under FCC unit conditions, Fuel Process. Technol. 192 (2019) 130–139, https://doi.org/10.1016/j.fuproc.2019.04.012.

[30] Z. Pan, X. Xue, C. Zhang, D. Wang, Y. Xie, R. Zhang, Evaluation of process parameters on high-density polyethylene hydro-liquefaction products, J. Anal. Appl. Pyrolysis 136 (2018) 146–152, https://doi.org/10.1016/j.jaap.2018.10.011.

[31] M.F. Ali, M.N. Siddiqui, S.S.H.H. Redhwi, M. Nahid, S.S.H.H. Redhwi, M.F. Ali, Study on the conversion of waste plastics/petroleum resid mixtures to transportation fuels, J. Mater. Cycles Waste Manag 6 (2004) 27–34, https://doi.org/10.1007/s10163-003-0102-x.

[32] H.K. Joo, C.W. Curtis, Effect of reaction time on the coprocessing of low-density polyethylene with coal and petroleum resid, Energy Fuels 11 (1997) 801–810, https://doi.org/10.1021/ef960158y.

[33] J. Weitkamp, Catalytic hydrocracking-mechanisms and versatility of the process, ChemCatChem 4 (2012) 292–306, https://doi.org/10.1002/cctc.201100315.

[34] E. Karakhanov, A. Maximov, Y. Kardasheva, M. Vinnikova, L. Kulikov, Hydrotreating of light cycle oil over supported on porous aromatic framework catalysts, Catalysts 8 (2018) 397, https://doi.org/10.3390/catal8090397.

[35] C.M. Halmenschlager, M. Brar, I.T. Apan, A. de Klerk, Hydrocracking vacuum gas oil with wax, Catal. Today 353 (2020) 187–196, https://doi.org/10.1016/j.cattod.2019.07.011.

[36] E. Stauffer, J.A. Dolan, Reta Newman, Flammable and Combustible Liquids, in: Handbook of Safety and Health for the Service Industry - 4 vol Set, CRC Press, London, 2020, pp. 199–233, https://doi.org/10.1201/b16087-54.

[37] C. Vasile, M.A. Brebu, T. Karayildirim, J. Yanik, H. Darie, Feedstock recycling from plastics and thermosets fractions of used computers. II. Pyrolysis oil upgrading, Fuel 86 (2007) 477–485, https://doi.org/10.1016/j.fuel.2006.08.010.

[38] X. Zhang, H. Lei, G. Yadavalli, L. Zhu, Y. Wei, Y. Liu, Gasoline-range hydrocarbons produced from microwave-induced pyrolysis of low-density polyethylene over ZSM-5, Fuel 144 (2015) 33–42, https://doi.org/10.1016/j.fuel.2014.12.013.

[39] M. Pan, J. Zheng, Y. Liu, W. Ning, H. Tian, R. Li, Construction and practical application of a novel zeolite catalyst for hierarchically cracking of heavy oil, J. Catal. 369 (2019) 72–85, https://doi.org/10.1016/j.jcat.2018.10.032.

[40] D.E. Romero, M. Rigutto, E.J.M. Hensen, Influence of the size, order and topology of mesopores in bifunctional Pd-containing acidic SBA-15 and M41S catalysts for n-hexadecane hydrocracking, Fuel Process. Technol. 232 (2022), 107259, https://doi.org/10.1016/j.fuproc.2022.107259.

[41] R. Palos, T. Kekäläinen, F. Duodu, A. Gutiérrez, J.M. Arandes, J. Jänis, P. Castaño, Detailed nature of tire pyrolysis oil blended with light cycle oil and its hydroprocessed products using a NiW/HY catalyst, Waste Manag. 128 (2021) 36–44, https://doi.org/10.1016/j.wasman.2021.04.041.

[42] W. Wang, X. Cai, H. Hou, M. Dong, Z. Li, F. Liu, Z. Liu, S. Tian, J. Long, Different mechanisms of coke precursor formation in thermal conversion and deep hydroprocessing of vacuum residue, Energy Fuels 30 (2016) 8171–8176, https://doi.org/10.1021/acs.energyfuels.6b01488.

[43] A. Gutiérrez, J.M. Arandes, P. Castaño, M. Olazar, J. Bilbao, Preliminary studies on fuel production through LCO hydrocracking on noble-metal supported catalysts, Fuel 94 (2012) 504–515, https://doi.org/10.1016/j.fuel.2011.10.010.

[44] V. Dagonikou, S. Bezergianni, D. Karonis, LCO upgrading via distillation and hydroprocessing technology, Energy Fuels 33 (2019) 1023–1028, https://doi.org/10.1021/acs.energyfuels.8b04024.

[45] P. Castaño, G. Elordi, M. Ibañez, M. Olazar, J. Bilbao, Pathways of coke formation on an MFI catalyst during the cracking of waste polyolefins, Catal. Sci. Technol. 2 (2012) 504–508, https://doi.org/10.1039/c2cy00434h.

[46] A. Ochoa, B. Aramburu, B. Valle, D.E. Resasco, J. Bilbao, A.G. Gayubo, P. Castaño, Role of oxygenates and effect of operating conditions in the deactivation of a Ni supported catalyst during the steam reforming of bio-oil, Green Chem. 19 (2017) 4315–4333, https://doi.org/10.1039/c7gc01432e.

[47] P. Castaño, A. Gutiérrez, I. Hita, J.M. Arandes, A.T. Aguayo, J. Bilbao, Deactivating species deposited on Pt-Pd catalysts in the hydrocracking of light-cycle oil, Energy Fuels 26 (2012) 1509–1519, https://doi.org/10.1021/ef2019676.

[48] F. Bauer, H.G. Karge, Characterization of coke on zeolites, in: Molecular Sieve, Science and Technology, Characterization II., Springer, Berlin, 2007, pp. 249–364, https://doi.org/10.5040/9781474217408.ch-005.

[49] M. Guisnet, P. Magnoux, Organic chemistry of coke formation, Appl. Catal. A Gen. 212 (2001) 83–96, https://doi.org/10.1016/S0926-860X(00)00845-0.

[50] B. Valle, P. Castaño, M. Olazar, J. Bilbao, A.G. Gayubo, Deactivating species in the transformation of crude bio-oil with methanol into hydrocarbons on a HZSM-5 catalyst, J. Catal. 285 (2012) 304–314, https://doi.org/10.1016/j.jcat.2011.10.004.

[51] K. Kohli, R. Prajapati, S.K. Maity, B.K. Sharma, Hydrocracking of heavy crude/residues with waste plastic, J. Anal. Appl. Pyrolysis 140 (2019) 179–187, https://doi.org/10.1016/j.jaap.2019.03.013.